

A&A manuscript no.  
(will be inserted by hand later)

Your thesaurus codes are:  
missing; you have not inserted them

# Direct Measurement of the Supernova Rate in Starburst Galaxies

J.D. Bregman<sup>1</sup>, P. Temi<sup>1</sup>, and D. Rank<sup>2</sup>

<sup>1</sup> NASA Ames Research Center, Moffett Field, CA 94035

email: jbregman@mail.arc.nasa.gov

email: temi@ssa1.arc.nasa.gov

<sup>2</sup> University of California Santa Cruz, Santa Cruz, CA 95064

email: rank@ucolick.org

Received ; accepted

**Abstract.** Supernovae play a key role in the dynamics, structure, and chemical evolution of galaxies. The massive stars that end their lives as supernovae live for short times. Many are still associated with dusty star formation regions when they explode, making them difficult to observe at visible wavelengths. In active star forming regions (galactic nuclei and starburst regions), dust extinction is especially severe. Thus, determining the supernova rate in the active star forming regions of galaxies, where the supernova rate can be one or two orders of magnitude higher than the average, has proven to be difficult. From observations of SN1987A, we know that the [NiII] 6.63  $\mu\text{m}$  emission line was the strongest line in the infrared spectrum for a period of a year and a half after the explosion. Since dust extinction is much less at 6.63  $\mu\text{m}$  than at visible wavelengths ( $A_{6.63}/A_V = 0.025$ ), the NiII line can be used as a sensitive probe for the detection of recent supernovae. We have observed a sample of starburst galaxies at 6.63  $\mu\text{m}$  using ISOCAM to search for the NiII emission line characteristic of recent supernovae. We did not detect any NiII line emission brighter than a  $5\sigma$  limit of 5 mJy. We can set upper limits to the supernova rate in our sample, scaled to the rate in M82, of less than 0.3 per year at the 90% confidence level using Bayesian methods. Assuming that a supernova would have a NiII with the same luminosity as observed in SN1987A, we find less than 0.09 and 0.15 per year at the 50% and 67% confidence levels. These rates are somewhat less if a more normal type II supernovae has a NiII line luminosity greater than the line in SN1987A.

**Key words:** Supernovae: general – galaxies: starburst

---

## 1. Introduction

While the supernova rate is one of the key parameters which constrain the initial mass function and rate of star formation in models of starburst galaxies, its value is difficult to measure (Doane and Mathews 1993). Observational approaches have been used to determine this rate, including observations of compact radio sources (Kronberg et al. 1985, Antonucci and Ulvestad 1988, Van Buren and Greenhouse 1994) and direct visible light imaging (Richmond et al. 1998). The radio observations suffer from confusion since there are a large number of point sources, and there is an uncertainty in the ages of the supernova remnants, leading to a range in the calculated supernova rate of 0.08-0.3 supernovae per year in M82. The optical observations did not detect any supernovae within the starburst regions of the observed galaxies, leading the authors to conclude that there was too much obscuration within the galaxies' nuclei to allow supernovae to be observed at visible wavelengths.

Van Buren and Norman (1989) suggested that supernovae in starburst galaxies could be directly observed in the infrared by imaging the galaxies in the [CoII]  $10.52\mu\text{m}$  emission line (from radioactive cobalt) since it would be a unique signature of a supernova and would provide information about the mass of the supernova. However, this line is exactly coincident with the  $10.52\mu\text{m}$  [SIV] emission line that is prevalent in planetary nebulae and HII regions. The [CoII] line, from  $\text{Co}^{56}$ , does decay with a half life of 77 days, so it would be possible to distinguish the difference between [SIV] and [CoII] lines by their temporal behavior if the [CoII] line was spatially separated from [SIV] line emission and it was a substantial fraction of the energy at  $10.52\mu\text{m}$ . Infrared spectra of SN1987A (Rank et al. 1988, Wooden et al. 1993) showed the [CoII] line in emission, but a [NiII] emission line, from  $\text{Ni}^{58}$ , at  $6.63\mu\text{m}$  was stronger and persisted longer than any other line. The emission lines appear after the peak of the visible light curve when the envelope becomes optically thin, about 120 days after the explosion. The [NiII] line was not evident in a spectrum obtained 60 days after the explosion, but was already a strong line at the next time of observation 260 days after the explosion. The line was weak but still visible at the last observation 775 days after the explosion. Thus, the [NiII] line should be visible in a supernova for nearly 2 years. This line is not seen in any other type of source, it is well separated from any other emission line, and is a unique and long lived supernova indicator which should be relatively free of obscuration from dust within the starburst nucleus.

With the launch of the Infrared Space Observatory (ISO), we were provided the opportunity to search nearby starburst galaxies for recent supernovae by imaging the galaxies at  $6.63\mu\text{m}$  and at several comparison continuum wavelengths. We did not detect any supernovae in the starburst nuclei, and to this date, no supernova has been detected

Table 1. Log of ISO Observations

<i>Name</i>	<i>Obs.Date</i>		<i>Int. Time</i> ( <i>sec.</i> )	<i>Num. of frames</i>
<i>IC342</i>	10/02/97	-	5.04	233
<i>NGC253</i>	06/07/97	-	5.04	155
<i>M82</i>	03/11/97	-	5.04	155
<i>NGC4449</i>	07/07/96	-	10.08	76
<i>NGC4945</i>	08/11/96	08/11/97	10.08	229
<i>NGC5128</i>	08/11/97	-	5.04	155
<i>NGC5236</i>	07/31/96	08/24/97	10.08	239
<i>CIRCINUS</i>	08/19/96	03/18/97	10.08	232
<i>NGC6946</i>	10/20/96	04/30/97	10.08	228
<i>NGC5055</i>	07/13/96	-	10.08	213

in a starburst nucleus. In this paper we derive a limit to the supernova rate in starburst nuclei from observations of a sample of galaxies. The observations and data reduction procedure are discussed in § 2, followed by a derivation of the supernova rate in § 3. Our results are summarized in § 4.

## 2. Observations and Data Analysis

Images of the galaxies listed in Table 1 were obtained with the infrared camera (ISO-CAM) aboard ISO. We were fortunate enough to get two epochs of observations for some of the galaxies, extending the coverage time by about a year. The first set of observations were made using a single set of continuously variable filter (CVF) settings with spectral resolution of  $\lambda/\Delta\lambda \simeq 45$ . In the second set of observations, we scanned the CVF from short to long wavelengths, moved the telescope 1.5 pixels, then scanned the CVF in the reverse direction. This provided us with redundant data, allowing us to better remove artifacts from internal reflections in the camera. We also found that the longest integration time (20 seconds) produced images with so many cosmic ray trails that it was nearly impossible to remove false signals. The same 10 CVF settings were used for all of the observations, and cover the wavelength range from  $6.04\mu\text{m}$  to  $7.795\mu\text{m}$ , including lines from [NiII] ( $6.63\mu\text{m}$ ), [ArII] ( $6.98\mu\text{m}$ ) and [Pfa] ( $7.45\mu\text{m}$ ) and adjacent continuum. For all of the observations we used the CAM04 AOT with 3 arcsec per pixel. A log of the observations is given in Table 1.

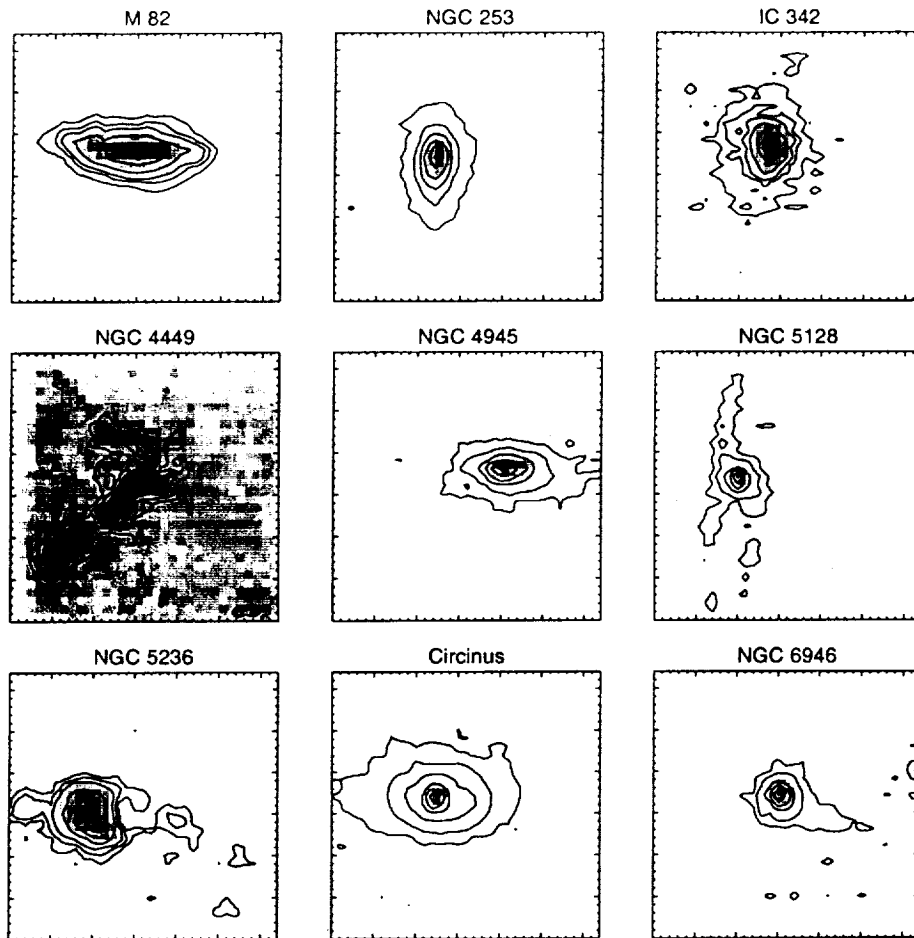


**Fig. 1.** Gray scale images of the galaxy sample at 6.63 μm overlaid with contour lines. Gray scale images are shown with the original 3 arcsec/pixel scale, while the contours have been smoothed with a 3 pixel FWHM gaussian filter. The lower contour in each galaxy is at a level equal to a noise of 5 σ.

### 2.1. Data Reduction

Data reduction has been performed using the Camera Interactive Analysis (CIA) package. The new release uses the latest calibration files available and some new algorithms for detector characterization and behavior. For the dark current subtraction, a *dark model* has been used to take into account the long term-drift in the dark current which occurred

during the ISO mission. Great effort has been devoted to removing cosmic ray hits on the detector. In order to detect a supernova event, we needed to generate continuum subtracted images of our target galaxies at  $6.63 \mu\text{m}$ . The galaxy's nucleus itself is a fairly bright point-like source, but the expected supernova signature is of the order of a few to tens of mJy. Thus, a clear detection on the subtracted frames relies heavily on the removal of cosmic rays and correction for the glitch-induced transient responses. Most of the short term duration glitches can be easily removed using a sigma clipping filter or the multi-resolution method. These glitches are produced by protons and electrons hitting the detector and their effects on the data are the typical spikes present on a pixel time history plot. The spike duration is shorter than the integration time and they last for no more than one or two readouts. Highly energetic protons and electrons and heavy ions are responsible for glitches that cannot be easily removed. These *special* glitches introduce a gain variation with a very long time constant. The gain stabilization can be very slow, and at the present time there is no method that corrects the effect in a satisfactory way. However, since we had redundancy in our data, we were able to check for remnants of long term response variations and either remove or mask these occurrences on the original CVF scan data frames.

The standard calibration file *cal-g* that comes along with the ISO data products is not very well suited for flat field correction with data taken with the CAM04 AOT. We built our own flat field combining calibration files that match our specific data set. After dark current correction, deglitching and stabilization, we can represent a set of data taken with the camera in the same configuration  $c$ , imaging a source on the array, as

$$I_{obs}(x, y, c) = F(\text{Source}(x, y) + \text{Zodiacal}(x, y)) \times \text{dflat}(x, y) \times \text{oflat}(x, y) + F(\text{Scatt}(x, y)) \times \text{dflat}(x, y) \quad (1)$$

The library flat field is separated in two distinct frames: the optical flat and the detector flat. Here,  $\text{Zodiacal}(x, y)$ ,  $\text{oflat}(x, y)$  and  $\text{dflat}(x, y)$  correspond to the Zodiacal light, the optical flat and the detector flat respectively as a function of pixel position  $(x, y)$ .  $\text{Scatt}(x, y)$  is the scattered light pattern which is produced inside the camera between detector and filter and is thus unaffected by the  $\text{oflat}(x, y)$ . We can re-write the same relation as

$$I_{obs}(x, y, c) = F(\text{Source}(x, y) \times \text{oflat}(x, y) \times \text{dflat}(x, y)) + \text{dflat}(x, y) \times \{F(\text{Zodiacal}(x, y)) \times \text{oflat}(x, y) + F(\text{Scatt}(x, y))\} \quad (2)$$

If the source does not produce too much scattered light,  $F(\text{Scatt}(x, y))$  can be ignored and the second term in equation (2) can be measured by scanning the zodiacal light. A good quality data cube for the zodiacal light, covering the entire CVF wavelength range, is not yet available. Using library CVF flat images, we built, by interpolation, a

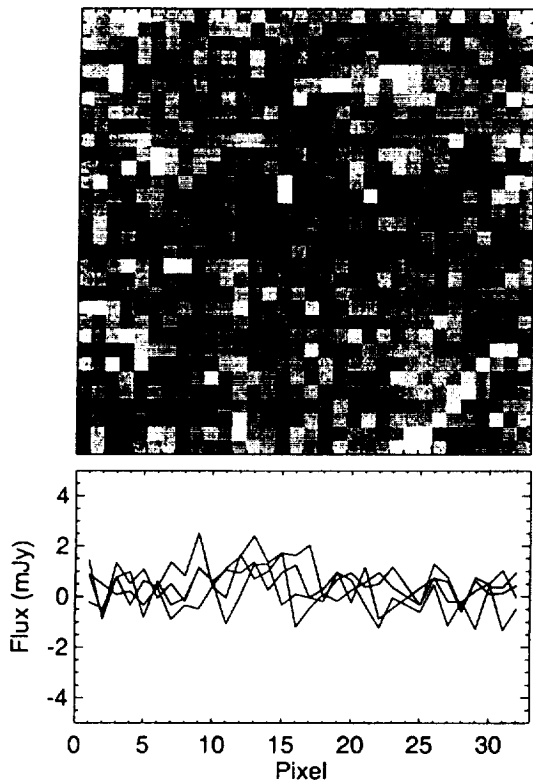


Fig. 2.  $6.63 \mu\text{m}$  continuum subtracted image of IC 342. Three row plots taken in the central region of the image show the peak to peak noise of the order of 3 mJy. A residual cosmic ray strip is seen in the lower right corner of the image.

datacube that matches the wavelengths in our measurements. Scaling this cube to the intensity measured off-source in our observations, and subtracting the scaled cube from the original data set, we are left with the  $F(\text{Source}(x, y)) \times oflat(x, y) \times dflat(x, y)$  term. The optical flat shows little structure in the central part of the array where our sources are centered. Thus there is no need to correct for it. This is not the case for the detector flat. We recovered some detector flats from the narrow band filter calibration files, and re-sampled them to match the wavelengths in our CVF scan. This way we created a detector flat cube we could use to flat field our data.

Figure 1 shows a panel of our galaxy sample. For each set of CVF scans we have produced  $6.63 \mu\text{m}$  continuum subtracted images; the  $1\sigma$  rms noise level on these maps is of the order of 0.8 mJy per pixel. Figure 2 displays a subtracted frame for IC 342 as an example of a fully reduced image. Low frequency noise from glitches is still the major contributor to the overall noise in the figure. If a possible detection were present in one frame, we had the opportunity to confirm the detection using the data taken with the CVF scanned in the opposite direction. We did not detect any clear emission from a supernova explosion in our sample using this criterium.

### 3. Discussion

#### 3.1. Comparison of [NiII] luminosity in SN1987A to a normal supernova

SN1987A is the only supernova bright enough to have been observed in the mid-infrared, and our knowledge of the [NiII] luminosity in supernovae is based solely on this one object. We therefore need to know how SN1987A compares to other Type II supernovae before we can determine the expected brightness of a supernova produced [NiII] line in other galaxies.

The radioactive tail of a supernova light curve is produced by thermalization of gamma rays from  $\text{Co}^{56}$  decay. The  $\text{Co}^{56}$  itself comes from rapid decay of the  $\text{Ni}^{56}$  produced in the supernova explosion. In most supernovae, almost all of the gamma rays are absorbed in the expanding envelope, so that the luminosity on the tail is a good indication of the amount of  $\text{Ni}^{56}$  produced by the supernova. Even though SN1987A did not achieve the peak luminosity of most Type II supernovae, it did have about the same luminosity as typical Type IIs after its peak (eg. Turatto et al. (1998)), and therefore had produced about the same amount of  $\text{Ni}^{56}$  as a typical Type II supernova, as expected from theoretical calculation of  $\text{Ni}^{56}$  production (see Figure 3).

The [NiII]  $6.63 \mu\text{m}$  line observed in SN1987A is a collisionally excited ground state forbidden line of  $\text{Ni}^{58}$ , which is also produced in the supernova explosion, and, like the bolometric luminosity, is powered by radioactive decay of  $\text{Co}^{56}$ . Gamma rays from the cobalt ionize the gas in the supernova envelope, heating the electrons. The [NiII] line intensity therefore depends on the density, on the quantity of  $\text{Ni}^{56}$  and  $\text{Ni}^{58}$  produced in the explosion, on the fraction of Ni and  $\text{Ni}^+$ , and on the temperature of the gas. The [NiII] line becomes visible when the optical depth in the expanding envelope becomes optically thin above the NiII zone, and is coincident with the start of the tail phase of a supernova. A typical Type II supernova takes 40-60 days to reach this phase, while the much slower expanding SN1987A took 120 days. However, the combined slower expansion and longer time results in the density of the NiII zone being about the same in SN1987A as in a typical type II. Also, due to the high density of the NiII emitting region, the [NiII]  $6.63 \mu\text{m}$  line intensity is only linearly dependent on the density. The amount of  $\text{Ni}^{56}$  and  $\text{Ni}^{58}$  produced as a function of mass and metallicity have been calculated by Woosley and Weaver (1995), and are plotted in Figure 3 for both solar and 0.1 solar metallicity. The LMC is about one third solar, so we would expect the Ni production to lie between these two curves. For comparison,  $0.075 M_{\odot}$  of  $\text{Ni}^{56}$  was produced by SN1987A, which agrees quite well with Woosley and Weaver calculations. A good indicator of the trend of the [NiII] emission line intensity is the product of  $\text{Ni}^{56}$  and  $\text{Ni}^{58}$ , which is shown in Figure 4. A supernova like SN1987A is near the minimum of the [NiII] line emission as a function

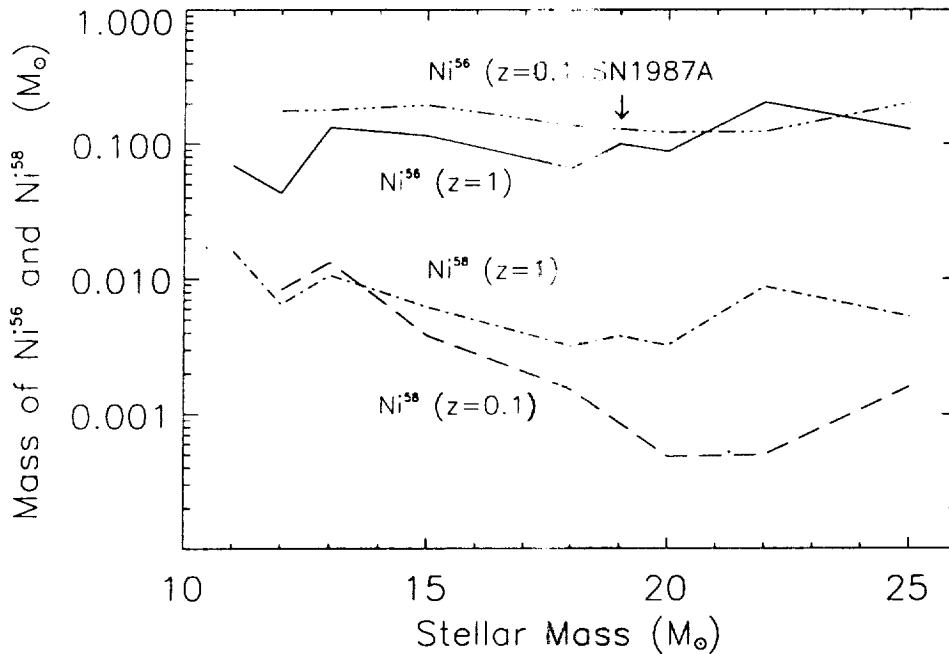


**Fig. 3.** The masses of  $\text{Ni}^{56}$  and  $\text{Ni}^{58}$  produced in a supernova explosion as calculated by Woosley and Weaver (1995) are shown as a function of stellar mass for both solar and 0.1 solar metallicity.  $\text{Ni}^{56}$  rapidly decays to  $\text{Co}^{56}$  which then produces the gamma rays that power the supernova during the tail phase when forbidden lines are visible.  $\text{Ni}^{58}$  is stable and is the source of the [NiII]  $6.63 \mu\text{m}$  emission line.

of mass, and significantly below that expected for a solar metallicity precursor. Thus, it is likely that the supernovae in galaxies with solar metallicities could have NiII emission lines from several times to an order of magnitude more luminous than that observed in SN1987A. In our [NiII] emission line estimates, we will use both the SN1987A value ( $6 \times 10^{-17} \text{ W cm}^{-2}$  Wooden et al. 1993) and a value 3 times greater than that observed in SN1987A. However, we should keep in mind that this value is very uncertain and we would learn a lot about NiII forbidden line emission if we observe just one supernova.

### 3.2. Visibility time for the sample

The measured [NiII] line intensity in SN1987A at four different epochs after the explosion (260, 415, 615 and 775 days) are reported by Wooden et al., (1993). The line intensity reaches its peak at 415 days after core collapse with an intensity of  $6.15 \times 10^{-17} \text{ W cm}^{-2}$ . At 775 days after collapse, the line intensity drops to  $4.37 \times 10^{-18} \text{ W cm}^{-2}$ , but is still the brightest emission line at infrared wavelengths. From these measurements we calculated the expected luminosity of a supernova occurring in each galaxy of the sample. The estimated peak signal that a supernova as bright as SN1987A would produce (in each



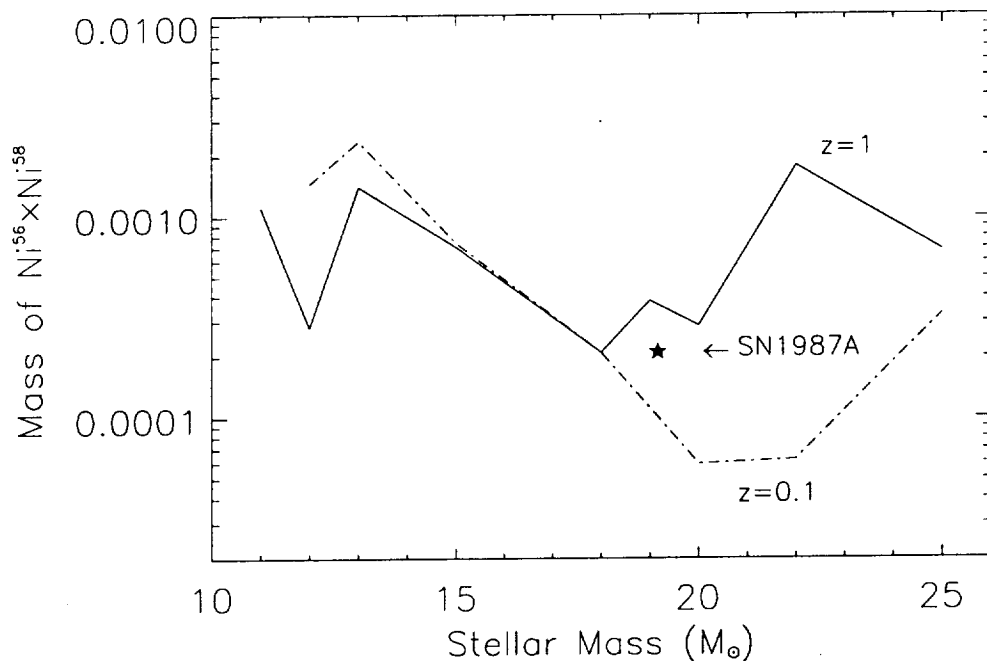
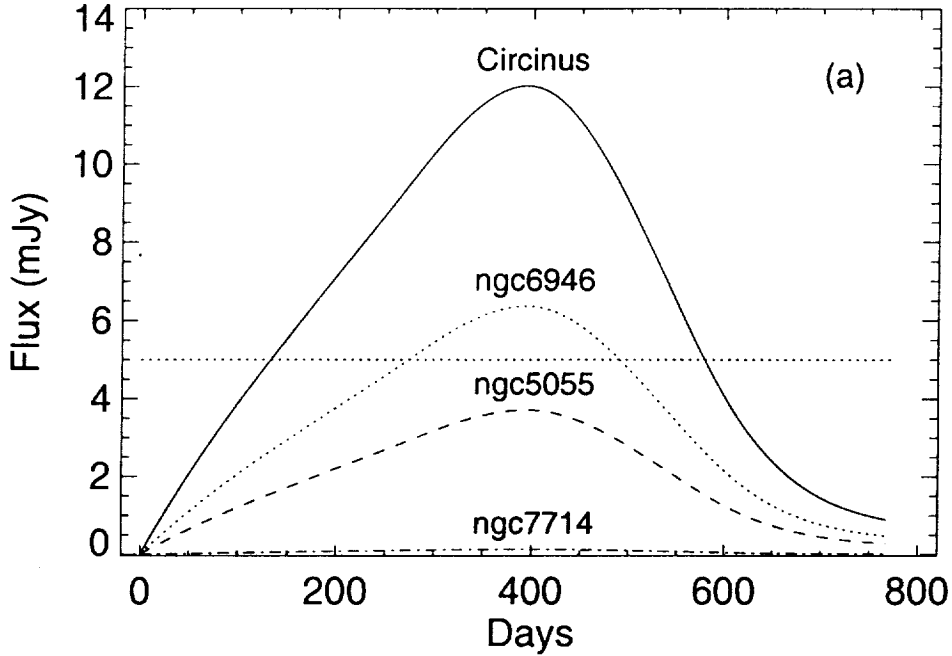


**Fig. 4.** The product of  $\text{Ni}^{56}$  and  $\text{Ni}^{58}$  is shown as function of stellar mass of a supernova progenitor for solar and 0.1 solar metallicity stars. Since  $\text{Ni}^{56}$  provides the gamma rays to power the supernova and the  $6.63 \mu\text{m}$  line is from  $\text{Ni}^{58}$ , their product is an indicator of how the  $[\text{NiII}] 6.63 \mu\text{m}$  line should vary with stellar mass and metallicity. The average solar metallicity supernova has a  $\text{Ni}^{56} \times \text{Ni}^{58}$  product 3-4 times that of SN1987A.

sample galaxy), is shown in figure 5. Since the noise level in the continuum subtracted maps is of the order of 0.8 mJy, we define a visibility time,  $t^{vis}$ , as the period of time in which the signal produced at  $6.63 \mu\text{m}$  by the  $[\text{NiII}]$  line would be  $\geq 5$  mJy, in each galaxy in our sample. This will allow us, in case of an event, to make a clear detection with a S/N ratio  $\geq 5$ . The visibility time in the sample ranges from  $\simeq 1$  year to more than 1.5 years for the closest galaxies; for a supernova with a NiII line emission 3 times brighter than SN1987A the visibility time for the sample increases by about 20%. For NGC 5055 the estimated signal from the NiII line, assuming a supernova as bright as SN1987A, never reaches the 5 mJy level required for a clear supernova detection with our data, while it has a visibility time of 1.2 years assuming a 3 times brighter supernova.

To take into account the fact that some of the galaxies have been observed twice during the ISO mission we need to compute the control time,  $C^{time}$ , reference for each galaxy of the sample defined as:

$$C_j^{time} = \sum_{i=1}^2 \Delta t_i \quad (3)$$



where:

$$\Delta t_i = \begin{cases} t_i^{vis} & \text{if } t_i - t_{i-1} \geq t_i^{vis} \text{ or } i = 1 \\ t_i - t_{i-1} & \text{if } t_i - t_{i-1} \leq t_i^{vis} \text{ and } i \neq 1 \end{cases} \quad (4)$$

Here  $t_i$  is the epoch of the  $i^{\text{th}}$  observation of the  $j^{\text{th}}$  galaxy. For those galaxies that have been observed only once, the control time  $C^{time}$  coincides with the visibility time  $t^{vis}$ . Control times are reported in column 5 of Table 2.

### 3.3. Derivation of the rate

In order to derive the supernova rate for our galaxy sample, we need some way of scaling the rates for the individual galaxies. Since the starburst nuclei are dusty, most of the energy produced by stars in the starburst will be absorbed by the dust and re-radiated at far infrared wavelengths. Thus, we can use the far infrared luminosities of the galaxies based on IRAS fluxes to scale the expected supernova rate for each galaxy (eg. Soifer et al. (1989)). This scaling will only be valid if the galaxy nuclei are optically thick in the visible, and if the FIR luminosity measured by IRAS is confined to the region we observe. For starburst galaxies, the starburst nucleus has a radius of a few hundred parsecs (Doane and Mathews, 1993). For M82, a 400 pc diameter starburst region extends for 25 arcsec, while our ISOCAM images extend for 90 arcsec. The galaxy images also show that the infrared emission is strongly concentrated near the nucleus.

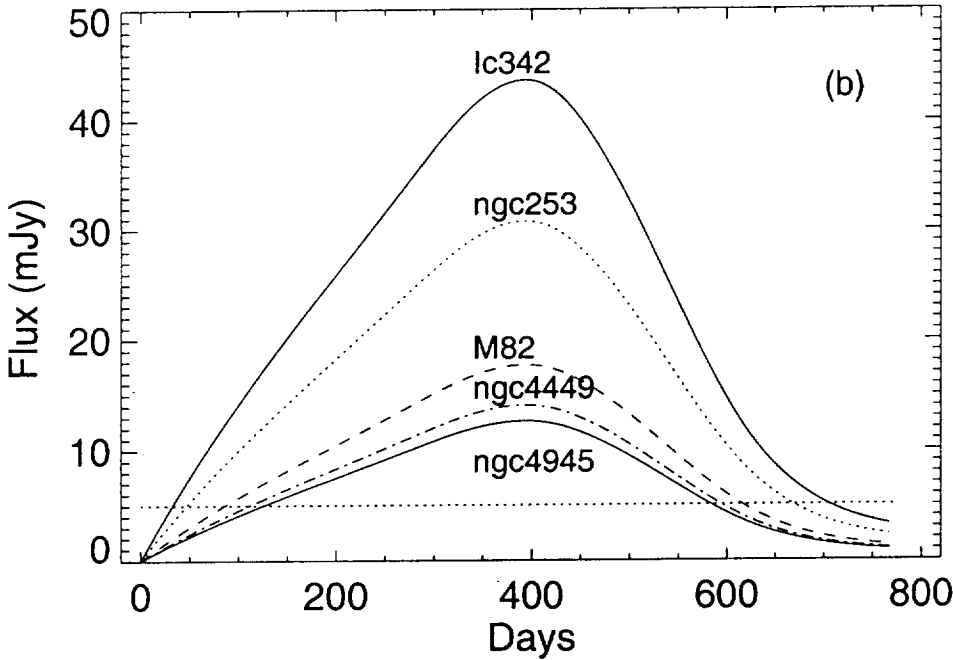


Fig. 5. Visibility time for the galaxy sample. The  $5\sigma$  limit for a supernova detection is shown as a dotted line. The expected NiII emission line intensities as a function of time after the explosion have been scaled from the measured intensity of SN1987A at different epochs.

From our data, we can derive a confidence level as a function of the supernova rate using Bayesian probabilities (see Sivia, 1996, for an excellent discussion of Bayesian data analysis). Bayes theorem is appropriate for data analysis where we have data and want to derive the probability of a model being true. In this case, the model is simply that supernovae occur randomly with a rate that gives the average time between supernovae which can be detected for a time  $\Delta t$  by observing the [NiII] emission line. The basic equation from Bayes theorem is usually stated as

$$\text{prob}(M|D, I) = \text{prob}(D|M, I) \times \text{prob}(M|I) \quad (5)$$

where  $M$  = the model,  $D$  = the data, and  $I$  = prior information, and all of the  $\text{prob}(\ )$  are probability density functions. The vertical bar means *given*, so the first term reads *the probability of the model given the data*. As with all probabilities, the total probability is one. The last term is the probability of the model being true given our knowledge of the model and the way our observing process occurs. Since we observe the galaxies at discrete times,  $t_{obs}$ , then we will only observe a supernova if it has occurred within a short time,  $\Delta t$ , before the observation. There are then two variables in our model, the supernova rate, which we will call  $\lambda$ , and the time during which a supernova could be detected,  $\Delta t$ . The probability of the data being true, which is that no supernova was seen, is 1 if the

Table 2. Control Times

<i>Name</i>	<i>d</i> <sup>a</sup> (Mpc)	<i>L<sub>FIR</sub></i> (10 <sup>10</sup> L <sub>⊙</sub> )	<i>SN Peak</i> (mJy)	<i>Control Time</i> (Days)	<i>Control Time(3σ)</i> <sup>b</sup> (Days)
<i>IC342</i>	2.1	0.23	43.62	667	759
<i>NGC253</i>	2.5	1.09	30.78	621	759
<i>M82</i>	3.3	1.98	17.66	529	705
<i>NGC4449</i>	3.7	0.08	14.05	483	667
<i>NGC4945</i>	3.9	1.75	12.64	825	1017
<i>NGC5128</i>	3.9	0.64	12.64	460	652
<i>NGC5236</i>	3.9	0.79	12.64	849	1041
<i>CIRCINUS</i>	4.0	1.20	12.02	656	855
<i>NGC6946</i>	5.5	0.83	6.36	406	763
<i>NGC5055</i>	7.2	0.53	3.71	0	429

<sup>a</sup> Distances for each galaxy in the sample are taken from the following authors: (Karachentsev et al.,1993)(IC 342), (Sreekumar et al., 1994)(NGC 253) (Doane and Mathews 1993)(M82), (Bajaja et al., 1994)(NGC 4449) (Bergman et al., 1992)(NGC 4945, NGC 5128, NGC 5236), (Curran et al., 1998)(Circinus) (Tully, 1988)(NGC 6946, NGC 5055), (Doane and Mathews 1993)(NGC 7714).

<sup>b</sup> Control Time based on a supernova with a NiII emission line 3 times brighter than SN11987A

observation occurred outside of the observing window and 0 if the observation occurred within  $\Delta t$  of the explosion. If the explosion occurs at  $t_1$ , then

$$\text{prob}(M|I) = \begin{cases} 1 & \text{if } t_1 + \Delta t < t_{obs} \\ 0 & \text{if } t_1 < t_{obs} < t_1 + \Delta t \end{cases} \quad (6)$$

We are then left with determining the  $\text{prob}(D | M,I)$ , or  $\text{prob}(D | \lambda, \Delta t)$ , which is the distribution of intervals between events which have a Poisson distribution, and is given by

$$P(\lambda, t) = \lambda e^{-\lambda t} \quad (7)$$

We are really interested in this probability integrated over time, keeping in mind that it is multiplied by  $\text{prob}(M | I)$ . Recalling that the total probability must equal 1, the normalized probability density function of interest is therefore

$$\text{prob}(M|D, I) = \Delta t e^{-\lambda \Delta t} \quad (8)$$

Our goal is to place an upper limit on the supernova rate from our data, and thus we should integrate this probability density function over all rates less than a maximum

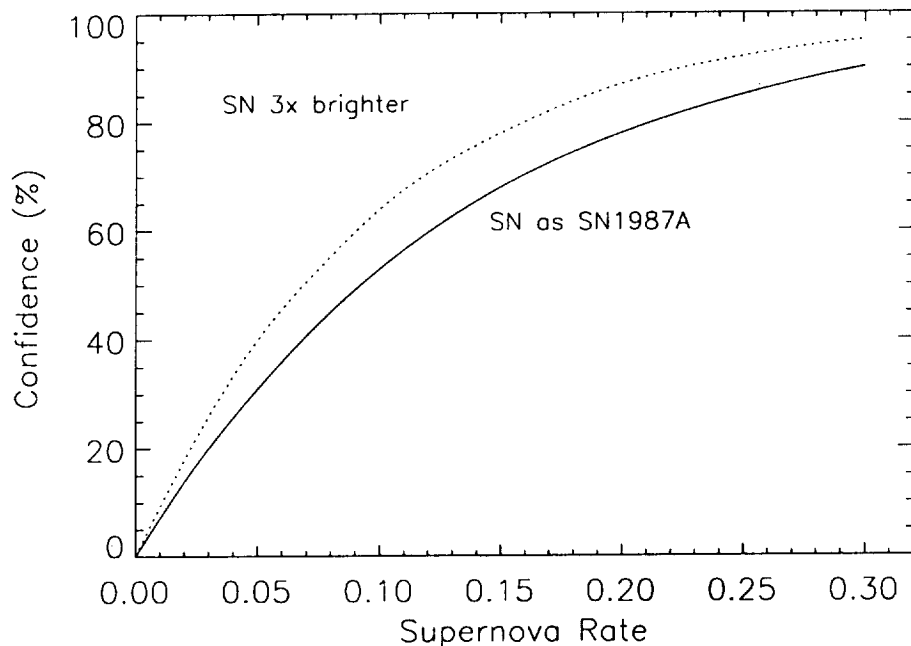


**Fig. 6.** The confidence (probability) of seeing a supernova in the galaxy sample as a function of the supernova rate in M82. The solid curve is for a supernova with a NiII line bright as SN1987A, while the dotted line assumes 3× brighter NiII line.

rate. Integrating over rates from zero to  $\lambda_m$  gives, for a single galaxy, the probability that the rate is less than  $\lambda_m$  of

$$P(\lambda < \lambda_m) = 1 - e^{(-\lambda_m \Delta t)} \quad (9)$$

For the complete sample of galaxies, we multiply the probabilities of not seeing a supernova in each galaxy when the rate is less than  $\lambda_m$ , then subtract that value from 1 to give the probability of seeing a supernova in our sample. Figure 6 shows the confidence (or probability) of seeing a supernova as a function of the maximum supernova rate for the entire galaxy sample scaled to M82 for both the SN1987A control time and the 3× SN1987A control time. The 50% confidence rate, that is the rate which has an equal probability of being correct or incorrect, is 0.09/0.065 supernovae per year in M82, where the first listed rate is for supernovae as bright as SN1987A. The 67% rate is 0.15/0.11 supernovae per year, while there is a 90% confidence that the rate is less than 0.30/0.23 supernovae per year in M82.

Supernova rates calculated by other authors are usually based on an approach which assumes a constant supernova rate. In that case, the probability of seeing a supernova is just the control time divided by the rate. This approach gives rates at fixed confidence levels which are somewhat less than we calculated using a Bayesian method, resulting

in rates of 0.09/0.065, 0.135/0.10, and 0.25/0.19 for confidence levels at 50%, 67%, and 90% respectively.

By comparison, Van Buren and Greenhouse (1994) derive a rate of 0.1 supernovae per year from radio source counts, assuming that all observed radio sources are supernova remnants, and modeling the evolution of the source brightness with time. They used data from Kronberg et al. (1985), who had derived a rate about twice their value, and quote a result of 0.2 per year from the evolution of radio sources observed by Kronberg and Sramek (1985). Doane and Mathews (1993) and Rieke et al. (1993) considered a supernova rate for M82 of between 0.1-0.3 as fitting the observational data. It is clear from our direct search for recent supernovae that the rate in M82 is highly unlikely to be greater than 0.2 per year, and it is doubtful that there are many supernovae hidden within dusty starburst nuclei or that there is any enhanced star formation in the galaxy cores.

#### 4. Summary

We have observed a sample of starburst galaxies at  $6.63 \mu\text{m}$  using ISOCAM to search for the NiII emission line characteristic of recent supernovae. While we did not detect any supernovae, we can put upper limits on the supernova rate. For example, the rate in M82 is less than 0.3 supernovae per year with a confidence of 90% assuming that the NiII line in a supernova will have the same luminosity as the line observed in SN1987A. For a supernova with a NiII line 3 times brighter than in SN1987A, the rate is less than 0.23 per year at the 90% confidence level. The corresponding rates for 50% and 67% confidence levels are 0.09/0.065 and 0.15/0.11 supernovae per year. There is thus no evidence in our data for an enhanced supernovae rate in the nuclei of starburst galaxies.

#### References

- Allen, M. L., and Kronberg, P. P. 1998, *ApJ*, 502, 218.
- Antonucci, R. R. J., and Ulvestad, J. S. 1988, *ApJ*, 330, L97.
- Bajaja, E., Huchtmeier, W.K., Klein, U., 1994, *A&A*, 285,385.
- Bergman, P., Aalto, S., Black, J. H., Rydbeck, G., 1992, *A&A*, 265, 403
- Cappellaro, E., Turatto, M., Tsvetkov, D., Bartunov, O. S., Pollas, C., Evans, R., Hamuy, M., 1997, *A&A*, 322, 431.
- Curran, S. J., Johansson, L. E. B., Rydbeck, G., Booth, R. S., 1998, *A&A*, 338, 863
- Doane, J. S., and Mathews, W. G 1993, *ApJ*, 419, 573.
- Karachentsev, I. D.; Tikhonov, N., 1993, *A&AS*, 100,227. Kronberg, P. P., Biermann, P., and Schwab, F. R. 1985, *ApJ*, 291, 693.
- Kronberg, P. P., and Sramek, R. A. 1985, *Science*, 227, 28.

- Rank, D. M., Pinto, P. A., Woosley, S. E., Bregman, J. D., Witteborn, F., Axelrod, T. S., and Cohen, M. 1988, *Nature*, 311, 505.
- Rice, W., Lonsdale, C. J., Soifer, B. T., Neugebauer, G., Kopan, E. L., Lloyd, L. A., De Jong, T. and Habing, H. J., 1988, *AJ*, 68, 91
- Richmond, M. W., Filippenko, A. V., and Galisky, J. 1998, *PASP*, 110, 553.
- Rieke, G. H., Loken, K., Rieke, M. J., and Tamblyn, P. 1993, *ApJ*, 412, 99.
- Sivia, A., *A Bayesian Tutorial*, Clarendon Press, Oxford 1996.
- Soifer, B. T., Boehmer, G., Neugebauer, G., and Sanders, D. B., 1989, *AJ*, 98, 776
- Sreekumar, P., Bertsch, D. L., Dingus, B. L., Esposito, J. A., Fichtel, C. E., Hartman, R. C., Hunter, S. D., Kanbach, G., Kniffen, D. A., Lin, Y. C., Mattox, J. R., Mayer-Hasselwander, H. A., Michelson, P. F., Von Montigny, C., Nolan, P. L., Schneid, E. J., Thompson, D. J., 1993, *ApJ*, 426, 105
- Tully, R.B., 1988, *Nearby Galaxies Catalog*.
- Turatto, M., Mazzali, P. A., Young, T. R., Nomoto, K., Iwamoto, K., Benetti, S., Cappellaro, E., Danziger, I. J., De Mello, D. F., Phillips, M. M., Suntzeff, N. B., Clocchiatti, A., Piemonte, A., Leibndgut, B., Covarrubias, R., Maza, J., Sollerman, J., 1998, *ApJ*, 498, L129.
- Van Buren, D., and Greenhouse, M. A. 1994, *ApJ*, 431, 640.
- Van Buren, D., and Norman, C. A. 1989, *ApJ*, 336, L67.
- Wooden, D. H., Rank, D. M., Bregman, J. D., Witteborn, F. C., Tielens, A. G. G. M., Cohen, M., Pinto, P. A., and Axelrod, T. S. 1993, *ApJS*, 88, 477.
- Woosley, S. E., and Weaver, T. A. 1995, *ApJS*, 101, 181.

